6th European Conference on Computational Mechanics (ECCM 6)
7th European Conference on Computational Fluid Dynamics (ECFD 7)
11 - 15 June 2018, Glasgow, UK

A COMPARISON OF METHODS FOR INTRODUCING SYNTHETIC TURBULENCE

Marcel Matha[1*], Christian Morsbach[1] and Michael Bergmann[1]

[1] German Aerospace Center (DLR)
Institute of Propulsion Technology
Linder Höhe, 51147 Cologne, Germany
marcel.matha@dlr.de, christian.morsbach@dlr.de, michael.bergmann@dlr.de

Key words: synthetic turbulence, source term, Large Eddy Simulation

Abstract. Scale resolving simulations are indispensable to provide in-depth knowledge of turbulence in order to improve turbulence modelling approaches for turbomachinery design processes. However, the inflow conditions of spatially evolving turbulent flow simulations are of utmost significance for the accurate reproduction of physics especially for Large Eddy Simulations. The present paper compares two approaches to introduce synthetically generated velocity fluctuations for Large Eddy Simulations: an inflow boundary condition and a source term formulation. In case of the boundary condition the velocity fluctuations are added to the mean velocity components at the inlet panel of the computational domain. The source term formulation uses an additional volume term in the momentum equation to add the fluctuating velocity field at an arbitrary location. The functionality of these methods in combination with the synthetic generation of fluctuations is validated in the generic test case of spatially decaying homogeneous isotropic turbulence. Furthermore, the spatial variation and anisotropy of turbulent statistics in a turbulent boundary layer as well as the development length of the different combinations, needed to reach a fully developed flow, are analysed for a turbulent channel flow.

1 INTRODUCTION

In order to design less noisy, more efficient and resource-conserving jet engines, the correct representation of turbulent flow structures in Computational Fluid Dynamics (CFD) is of crucial importance. Since Reynolds-averaged Navier-Stokes (RANS) modelling is prone to show inaccuracies in regions where strong streamline curvature, separation, transition, relaminarization and heat transfer play a role, scale resolving simulations are indispensable [1]. Despite the enormous increase in computational power, scale resolving simulations, e.g. Direct Numerical Simulations (DNS) and Large Eddy Simulations (LES), will not be part of the industrial design process in the coming decades. Nevertheless, through the gains in knowledge of turbulence provided by LES, which are a compromise between accuracy and computational costs, RANS models in industrial application will continuously be enhanced.

However, the prescribed inflow conditions of spatially evolving turbulent flow simulations are of utmost importance for the accurate reproduction of physics for LES. Tabor and Baba-Ahmadi [2] distinguish between two different approaches in order to obtain adequate inflow conditions including turbulent fluctuations. On the one hand, there is the Precursor Simulation Method, in which the inflow conditions are created performing a separate precomputation. Due to the fact that such an approach is not always feasible for industrial applications, another procedure based on statistical quantities such as Reynolds stresses and integral values, called Synthetic Turbulence Generator (STG), emerged. The goal of an STG is the synthetical generation of velocity fluctuations with respect to the correct representation of integral quantities like length and time scales. The mapping of the characteristic turbulent energy cascade characterized by coherent vortex structures is essential in order to judge the functionality of these methods. Furthermore, a practice-oriented STG should be able to reproduce the isotropy of turbulence as well as the anisotropy in a turbulent boundary layer. Druault et al. [3] show that synthetically generated velocity fluctuations, which simply follow a Gaussian distribution, consequently lacking any fluid mechanics background, are not able to reproduce the expected turbulent flow field. Therefore, the supply of correct spatial and temporal correlations for the STG is the key for the occurrence of fully evolved, realistic turbulent structures. A decisive criterion for the valuation of an STG is the development length, which characterizes the covered distance of the flow before realistic turbulence is established. There are many STG approaches to fulfil the criteria mentioned above. Keating et al. [4], e.g., review different methods of prescribing inflow conditions for LES.

In this paper we employ the STG suggested by Shur et al. [5], based on Fourier reconstruction of the fluctuating velocity field using wave vectors with uniformly distributed random directions. The goal of this paper is to compare two approaches for introducing the synthetically generated velocity field into the CFD domain: an inflow boundary condition and a source term formulation. In case of the boundary condition the velocity fluctuations are added to the mean velocity components at the inlet panel of the computational domain. The volume source term by Schmidt and Breuer [6], which was originally combined with an STG method based on a digital filter concept, uses an additional source term in the momentum equation to add the fluctuating velocity field at the desired location in the volume. This numerical flexibility results in the possibility to use coarser grids upstream of the source term location due to the absence of turbulent fluctuations.

This paper is organized as follows: First, the theory of the applied Fourier-technique is outlined. The two approaches to introduce the fluctuations generated by the STG are stated subsequently. Section 3 presents the simulation results, before the last section summarizes the results and issues an outlook.

2 NUMERICAL METHODS

The synthetic generation of turbulent fluctuations is performed using the parallelized multi-block CFD-solver TRACE, which is being developed by the DLR's Institute of Propulsion Technology with focus on turbomachinery [7]. TRACE solves the compressible, unsteady filtered Navier-Stokes equations according to the LES approach. In this

context we use the cell-centred finite-volume method, whereby a fraction of $\phi = 10^{-3}$ of Roe's numerical flux [8] is added to a central flux. Second order accuracy for the advective fluxes is achieved by applying van Leer's MUSCL extrapolation [9] as well as for the viscous fluxes via a central finite difference scheme. An explicit Runge-Kutta algorithm with third order accuracy is used to obtain precise and robust time integration for the unsteady computations. The general concept of the STG of Shur et al. [5], which employs ideas of Kraichnan [10], is described in the following, whereupon the two methods to introduce the synthetically generated fluctuations into the flow field are discussed.

2.1 Synthetic turbulence generation

The parts of the formulation of the STG stated here, are important to understand the general concept to obtain turbulent velocity fluctuations. For detailed explanatory notes on this approach, the reader is referred to the original publication [5].

Similarly to the statistical turbulence modelling the velocity vector can be split in a mean velocity $\widetilde{\mathbf{u}}(\mathbf{r})$ and a synthetically generated fluctuating part $\mathbf{u}''_{\text{syn}}(\mathbf{r}, t)$. The velocity at a point $\mathbf{r} = \{x, y, z\}$ reads:

$$\mathbf{u}(\mathbf{r}, t) = \widetilde{\mathbf{u}}(\mathbf{r}) + \mathbf{u}''_{\text{syn}}(\mathbf{r}, t) \tag{1}$$

A transformation is used to express the velocity fluctuations in Equation (1):

$$u''_{\text{syn},i}(\mathbf{r}, t) = a_{ij} v''_j(\mathbf{r}, t) \tag{2}$$

By means of the introduction of the fluctuating vector $\mathbf{v}''$, which satisfies the restrictions $\widetilde{v''_j} = 0$ and $\widetilde{v''_i v''_j} = \delta_{ij}$, the Reynolds stresses are correct owing to the definition of the tensor $\mathbf{A}$. The Cholesky decomposition of the Reynolds stress tensor, $\tau_{ij} = \mathbf{A}\mathbf{A}^T$, leads to:

$$\mathbf{A} = \{a_{ij}\} = \begin{pmatrix} \sqrt{\tau_{xx}} & 0 & 0 \\ \tau_{yx}/a_{xx} & \sqrt{\tau_{yy} - a_{yx}^2} & 0 \\ F\tau_{zx}/a_{xx} & \left(\tau_{zx} - a_{yx}a_{zx}\right)/a_{yy} & \sqrt{\tau_{zz} - a_{zx}^2 - a_{zy}^2} \end{pmatrix} \tag{3}$$

In order to determine the velocity fluctuation in Equation (2) the fluctuating vector $\mathbf{v}''$ has to be computed:

$$\mathbf{v}''(\mathbf{r}, t) = 2\sqrt{\frac{3}{2}} \sum_{n=1}^{N} \sqrt{q^n} \left[\sigma^n \cos\left(k^n \mathbf{d}^n \cdot \mathbf{r}' + \phi^n\right)\right] \tag{4}$$

Here:

- N is the number of modes
- q^n is the normalized amplitude of the mode n, defined by the local energy spectrum and determined from a modified von-Karman spectrum
- $\mathbf{d}^n$ is a random unit vector of direction uniformly distributed over a sphere
- k^n is the amplitude of the wave vector of the mode n: $\mathbf{k}^n = k^n \mathbf{d}^n$

- σ^n is a unit vector normal to $\mathbf{d}^n$ ($\sigma^n \cdot \mathbf{d}^n = 0$)
- ϕ^n is the phase of the mode n (random number, uniformly distributed in $[0, 2\pi)$)

As all quantities in Equation (4) are defined only once before the start of the simulation, there is no time-dependency so far. Thus, Shur et al. [5] propose the use of a pseudo-position vector

$$\mathbf{r}' = \begin{pmatrix} x' \\ y' \\ z' \end{pmatrix} = \begin{pmatrix} \frac{2\pi}{k^n \max\{l_e(\mathbf{r})\}} \left(x - u_{\text{macro}} t\right) \\ y \\ z \end{pmatrix} \quad , \tag{5}$$

whereby u_{macro} represents a macro-scale velocity.

2.2 Inflow formulation of the STG

The synthetically generated velocity fluctuations in Equation (2) are added to the mean velocity component in the respective direction according to Equation (1). The superposition takes place at the inlet of the computational domain, resulting in a Dirichlet boundary condition for the simulation.

2.3 Source term formulation of the STG

As the source term formulation is based on the concept of Schmidt and Breuer [6], which uses an additional source term S_{syn,u_i} in the momentum equation, the reader is again referred to the original publication for all details of the approach.

Subtracting the initial momentum equation from the modified one including the additional source term, while assuming that the advective and diffusive fluxes do not change because of the introduction of this term, yields the formulation of the source term:

$$\int_V S_{\text{syn},u_i} \, dV = \int_V \frac{\partial \left[\rho u''_{\text{syn},i}\right]}{\partial t} \, dV \tag{6}$$

In order to avoid rapid relaminarization the time derivative in Equation (6) is replaced by the integral time scale T_T:

$$\int_V S_{\text{syn},u_i} \, dV = \int_V \frac{\left[\rho u''_{\text{syn},i}\right]}{T_T} \, dV \tag{7}$$

Additionally, the time scale can be interpreted as a relaxation time needed to react to disturbances, hence the time step should be much smaller ($\Delta t \ll T_T$) preventing a rapid and strong system response. Moreover, to avoid discontinuities and ensure a fast spatial development of turbulent structures, the amplitude of the source term is scaled with a Gaussian distribution according to the streamwise distance $d = |x - x_{ST}|$ to the origin of the source term x_{ST} and the integral length scale L_T:

$$S^{CFD}_{\text{syn},u_i}(x) = S_{\text{syn},u_i} \cdot \underbrace{\exp\left(-\frac{\pi d^2}{2L_T^2}\right)}_{\text{G}} \tag{8}$$

Based on the Taylor's hypothesis for $\widetilde{u}_i \gg u_i''$, the integral time scale is computed using the streamwise velocity component u_x and the integral length scale:

$$T_T = \frac{L_T}{u_x} \tag{9}$$

The source term S_{syn,u_i} is calculated at x_{ST} for each time step and distributed in streamwise direction according to the exponential function G.

3 RESULTS & DISCUSSION

The inflow and source term formulation in combination with the STG, described above, are investigated in the generic test case of spatially decaying homogeneous isotropic turbulence and a turbulent channel flow application.

3.1 Spatially decaying homogeneous turbulence

The fundamental functionality of the STG in combination with the methods to introduce the fluctuations into the CFD domain is evaluated by a spatially decaying homogeneous turbulence test case. The test case with a Mach number of 0.1 features periodic boundary conditions perpendicular to the streamwise direction. Thus, lacking any shear layer and production of turbulence after adding the synthetically generated turbulent fluctuations, the spatial decay takes place. Multiples of the turbulent length scale, $8\pi L_T \times 2\pi L_T \times 2\pi L_T$ with $L_T = 0.001$m, represent the domain size discretized on a mesh of $128 \times 32 \times 32$ rectangular hexahedra. The origin of the source term is located at $x_{ST} = \frac{1}{16} L_x$. One axial through-flow of the domain is resolved with 2304 time steps. After two through-flows the averaging of the flow variables starts, while 22 through-flows are simulated. The subgrid stresses are computed by the Smagorinsky model [11].

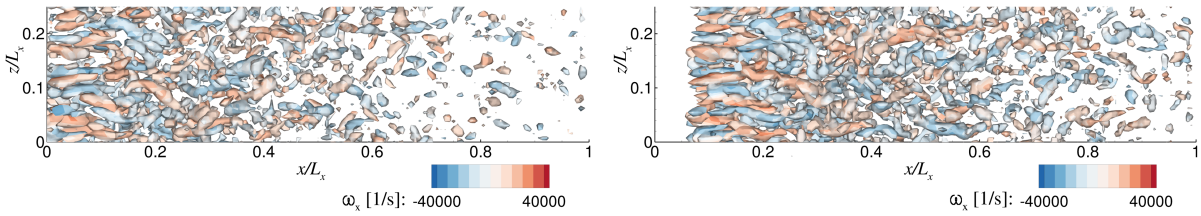

(a) Inflow formulation

(b) Source term formulation

Figure 1: Spatial development of vortex structures illustrated by isosurface $\lambda_2 = -0.0025$ and streamwise vorticity component in XZ-plane

The difference in the functionality is illustrated in Figure 1. Whereas vortex structures are only present downstream of the source term position in picture 1(b), the inflow formulation leads to an immediate decay of vortex structures from $x/L_x = 0$ onwards. Furthermore, it is observed that the inflow formulation introduces less turbulence kinetic energy compared to the source term formulation, see Figure 2 and Figure 3. Whereby $\Delta x = x - x_{ST}$ represents the relative distance referred to the source term origin. However,

the STG does not generate fully isotropic turbulence as specified by the input parameters. With increasing distance from the location, where the superimposition of the turbulent fluctuations to the flow field takes place, the differences between the normal stresses return to isotropy, also indicated by the convergence to zero of the shear stress components, due to the absence of velocity gradients.

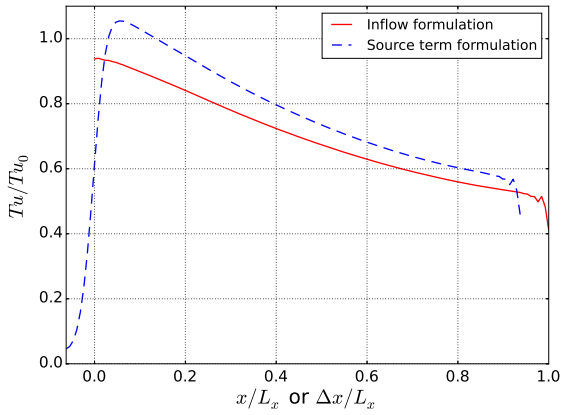

Figure 2: Turbulence intensity with reference to input parameter Tu_0

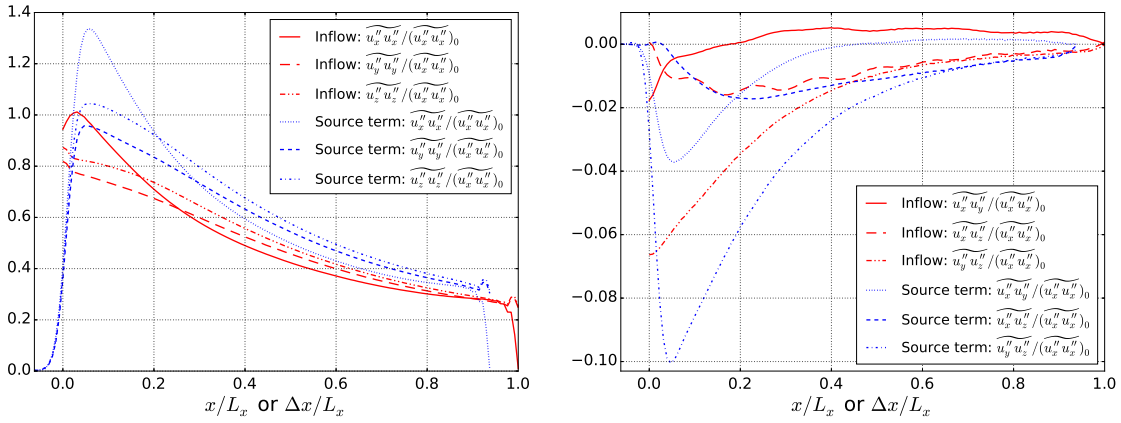

(a) Normal stresses

(b) Shear stresses

Figure 3: Reynolds stresses with reference to input Reynolds stress $(\widetilde{u_x''u_x''})_0$

Based on simulations with 10 times the simulation duration as before, respectively 220 through-flows, energy spectra resulting from autocorrelations are computed. Figure 4 shows the Fourier transform of the autocorrelations, i.e. the Power Spectral Density (PSD), at constant locations. Both formulations lead to an early evolution of the characteristic spectrum, as the $-5/3$ law in the inertial range is already recognizable at $x/L_x \approx 0,18$, respectively $\Delta x/L_x \approx 0,18$. With increasing distance covered the inertial

range becomes even pronounced, because of the evolution from superimposed, synthetically generated fluctuations to physical turbulent structures.

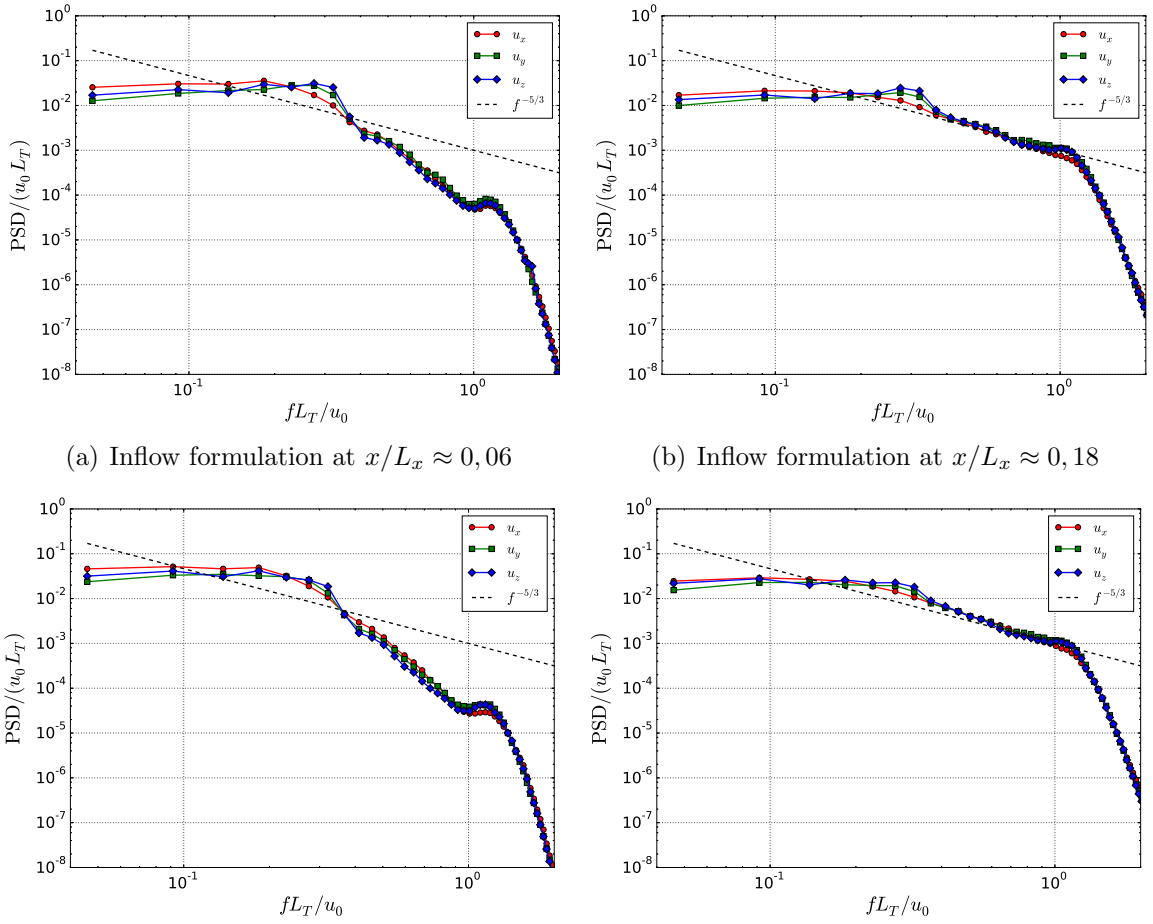

(a) Inflow formulation at $x/L_x \approx 0,06$

(b) Inflow formulation at $x/L_x \approx 0,18$

(c) Source term formulation at $\Delta x/L_x \approx 0,06$

(d) Source term formulation at $\Delta x/L_x \approx 0,18$

Figure 4: PSD scaled with input velocity u_0 and turbulent length L_T of the spatially decaying turbulence

3.2 Channel flow

In order have a look at the spatial variation and anisotropy of turbulent statistics in a turbulent boundary layer, the STG is applied in a turbulent channel flow. To enforce the Reynolds number based on the friction velocity $Re_\tau = 395$, a constant body force source term in the streamwise momentum equation is used. In order to minimize compressibility effects, the Mach number is set to 0.1. A reference solution, which is the result of a periodic channel, is required to investigate the development length of the STG in a finite-dimensional channel flow application. Therefore, the computational domain of the periodic channel is set up with periodic boundaries in streamwise direction as well as in z-direction. The domain size is defined by multiples of the channel half-height $\delta = 0.006$m. For the periodic case this results in $2\pi\delta \times 2\delta \times \pi\delta$ on a mesh of $72 \times 54 \times 72$ rectangular

hexahedra. The finite-dimensional channel is 5 times longer and has $360 \times 54 \times 72$ cells. The corresponding grid steps in wall units are $\Delta x^+ \approx 34$, $\Delta z^+ \approx 17$, $\Delta y^+_{\text{min}} \approx 0.6$ and $\Delta y^+_{\text{max}} \approx 35$, whereby the grid resolution was chosen on the basis of a compromise between accuracy and computational costs. The origin of the source term is located at $x_{ST} = \frac{1}{10} L_x$. In case of the periodic channel, the whole domain is initialized by the superimposition of the velocity fluctuations generated by the STG and the mean velocity components, while the inflow and source term formulation is applied to the finite-dimensional channel. Based on the investigations of Bergmann et al. [12] a statistical averaging of the flow variables takes place after a transient phase of 20 eddy turnover times $ETT = tu_\tau/\delta$. Both cases are resolved with 40 ETT, resulting in approx. 50 through-flows in the periodic case and approx. 20 through-flows in the finite case. The WALE model is applied in order to obtain the subgrid stresses for the LES [13].

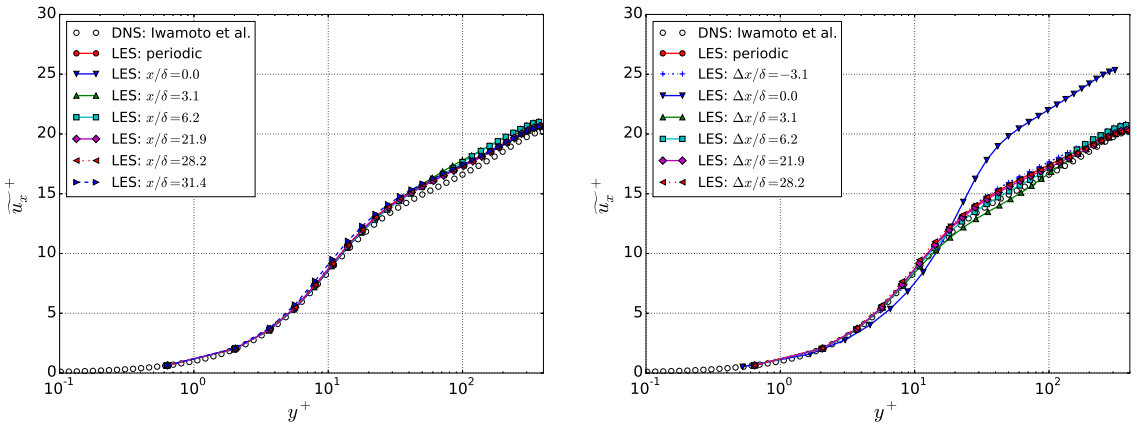

(a) Inflow formulation (b) Source term formulation

Figure 5: Development of velocity profiles in streamwise direction

Hereinafter, the spatially evolving LES results labelled with a specification of location are compared with the solution of the periodic channel and incompressible DNS results of Iwamoto et al. [14]. The streamwise velocity profile scaled with the friction velocity $\widetilde{u_x}^+ = \widetilde{u_x}/u_\tau$ shows agreement in the viscous sublayer with the DNS results, whereas the differences become larger in the log-law region, see Figure 5. Starting from the initialization by the averaged periodic solution, the velocity profiles of the inflow formulation in Figure 5(a) tend to greater values as far as $x/\delta \approx 5$, where this effect is eventually reversed yielding convergence to the periodic solution. This turning point can be identified as the minimum in the friction coefficient in Figure 6. Based on the comparison with the periodic solution, the development length of the inflow formulation is determined to $20x/\delta$. Keating et al. [4] identified a similar development length for an STG based on Batten et al. [15], which is also a modified version of the method proposed by Kraichnan [10]. By employing a zonal RANS-IDDES (Improved Delayed Detached Eddy Simulation) approach, Shur et al. [5] stated a shorter development length of their own STG.

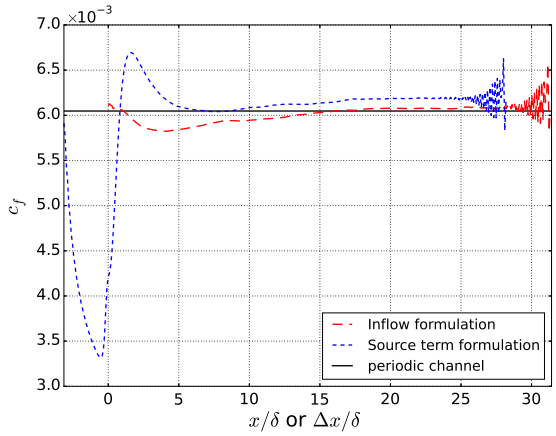

Figure 6: Comparison of the friction coefficient

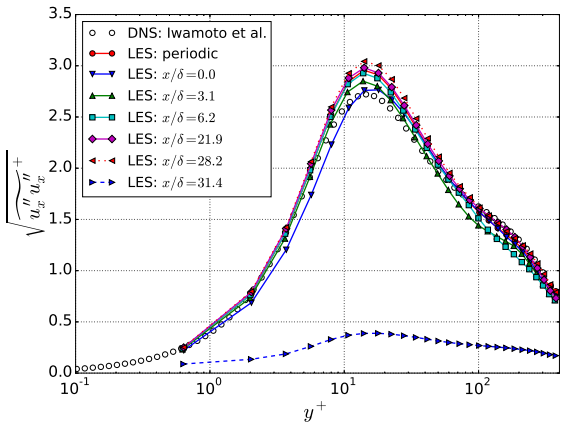

(a) RMS of turbulent velocities $\sqrt{\widetilde{u_x''u_x''}}^+$

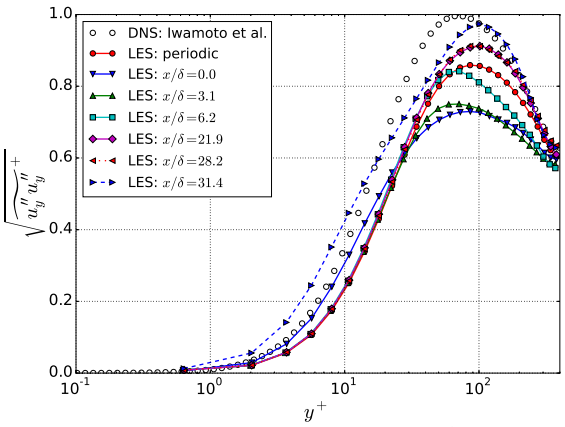

(b) RMS of turbulent velocities $\sqrt{\widetilde{u_y''u_y''}}^+$

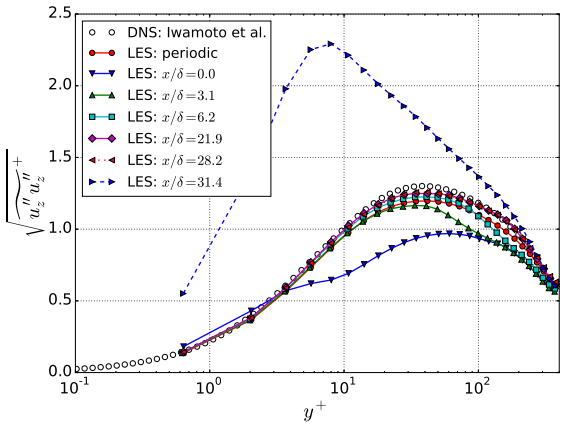

(c) RMS of turbulent velocities $\sqrt{\widetilde{u_z''u_z''}}^+$

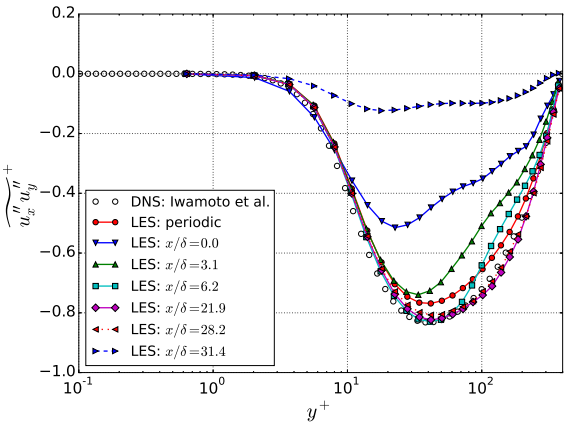

(d) Shear stress $\widetilde{u_x''u_y''}^+$

Figure 7: Development of Reynolds stresses in streamwise direction for the inflow formulation

When having a look at the Reynolds stresses in Figure 7, whereby

$$\widetilde{u_i'' u_j''}^{+} = \widetilde{u_i'' u_j''}/u_\tau^2 \quad , \tag{10}$$

the overestimation of the velocity profile can also be recognized by the root mean square (RMS) of the streamwise velocity fluctuations. In general the Reynolds stresses increase with covered distance ending in no realistic results at $x/\delta > 28.5$, respectively $\Delta x/\delta > 25.4$ for the source term approach. The shape of these last profiles is due to the effect of the exit boundary condition. The streamwise velocity profile of the source term formulation differs extremely from the DNS results next to $\Delta x/\delta = 0$, i.e. approximately the source term position x_{ST}. This is because of the formation of a laminar velocity profile out of the prescribed turbulent one without fluctuations, identified as the drop in friction coefficient upstream of the source term location in Figure 6. The synthetically generated fluctuations tend to laminarize directly after adding to the flow field, as the decrease in shear stress

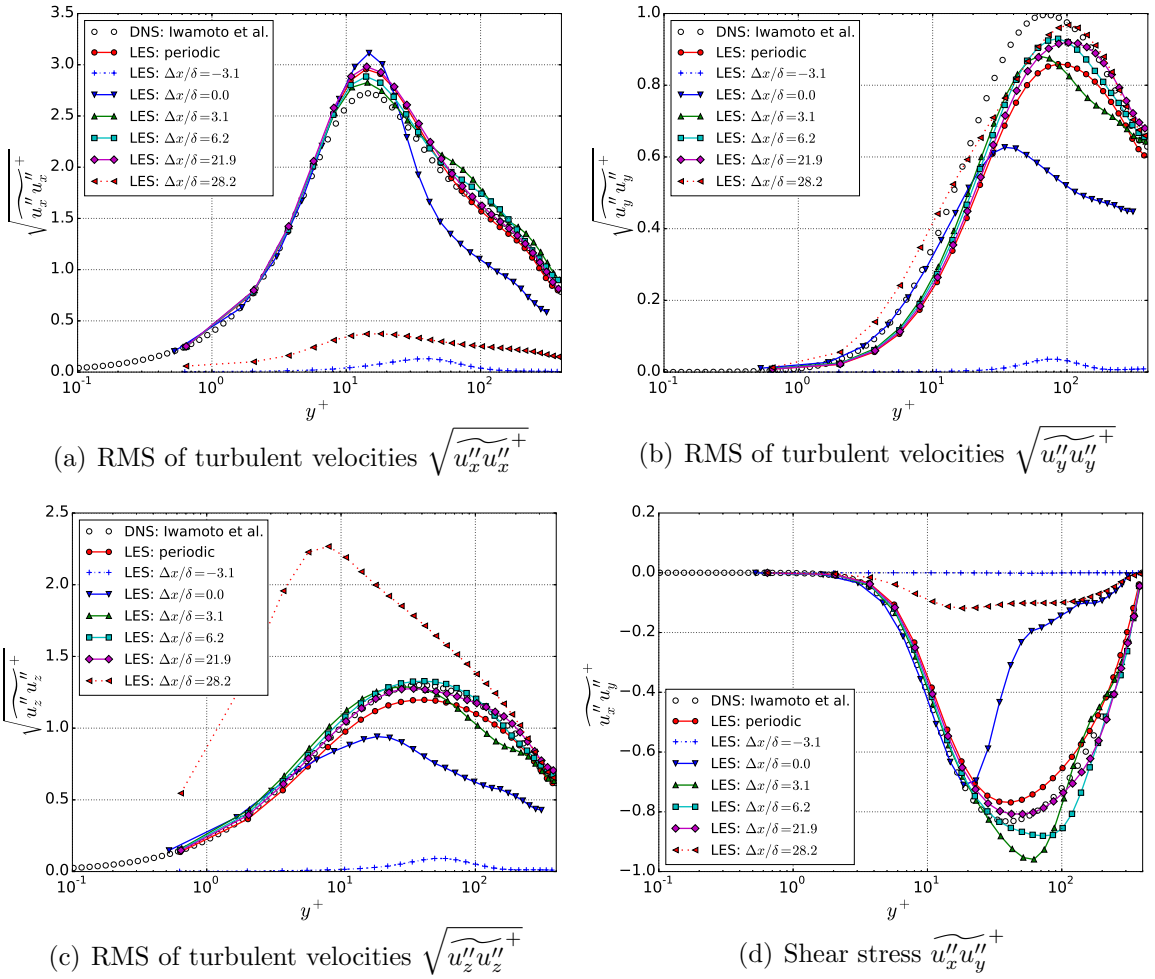

(a) RMS of turbulent velocities $\sqrt{\widetilde{u_x'' u_x''}^{+}}$

(b) RMS of turbulent velocities $\sqrt{\widetilde{u_y'' u_y''}^{+}}$

(c) RMS of turbulent velocities $\sqrt{\widetilde{u_z'' u_z''}^{+}}$

(d) Shear stress $\widetilde{u_x'' u_y''}^{+}$

Figure 8: Development of Reynolds stresses in streamwise direction for the source term formulation

can also be recognized downstream of the superimposition for the inflow formulation. Going across the source term position, an increase of friction resulting in an overshoot is observed. Subsequently, the friction coefficient reaches a plateau, so that the source term formulation features the same development length of $20\Delta x/\delta$ as the inflow formulation. Schmidt and Breuer [6] present a similar development length and progression in friction coefficient for the source term formulation applied to hybrid simulations (RANS-LES). The overestimation of the fully developed friction coefficient compared to the periodic solution, can be seen in [6] as well. Furthermore, it is noticeable that the LES results in close vicinity to the source term position have the smallest discrepancy to the velocity profile of the DNS at $y^+ < 70$, whereas the longer the distance from the source term location the better the approximation holds for $y^+ > 70$. In contrast to the inflow formulation, the Reynolds stresses of the source term formulation, illustrated in Figure 8, indicate that there is no turbulence kinetic energy upstream of the source term location, as the flow field has not experienced the total impact of the source term yet. Downstream of the source term origin the stresses develop due to the formation of a boundary layer associated with the production of turbulence in the same way as they do when applying the inflow formulation. In comparison to the inflow formulation, the normal stress component in z-direction and the shear stress of the source term formulation coincide better with the DNS results, while there is no difference with reference to accordance in x- and y-direction of the normal stresses.

4 CONCLUSIONS

In this work, we investigated the performance of the STG by Shur et al. [5] in combination with two approaches to introduce the fluctuations into the flow field. The inflow and the source term formulation, based on Schmidt and Breuer [6], showed very similar results in the isotropic as well as in the anisotropic, wall-bounded test case, confirming their functionality. Thus, the STG in combination with the inflow or the source term formulation is capable to represent the turbulent energy spectrum as well as the turbulent boundary layer profiles of streamwise velocity and second-order moments. One benefit of the source term formulation is the opportunity to apply existing non-reflecting boundary conditions without modification, whereas the inflow formulation requires an adaption of the inlet boundary condition to superimpose the fluctuations. Moreover, since the source term formulation provides the flexibility to introduce turbulent fluctuations at an arbitrary position in the flow field, where the grid is sufficiently fine and consequently the damping of small turbulent structures is negligible, this method should be considered for future simulations requiring turbulent fluctuations in the inflow for turbomachinery applications.

REFERENCES

[1] Tyacke, J.C. and Tucker, P.G. Future Use of Large Eddy Simulations in Aero-engines. *ASME Journal of Turbomachinery,* 137(8):081005-081005-16, 2015

[2] Tabor, G.R. and Baba-Ahmadi, M.H. Inlet conditions for large eddy simulation: A review., *Computers & Fluids,* 39(4), pp. 553-567, 2009

[3] Druault, P. and Lardeau, S. and Bonnet, J.-P. and Coiffet, F. and Delville, J. and Lamballais, E. and Largeau, J.F. and Perret, L. Generation of Three-Dimensional Turbulent Inlet Conditions for Large-Eddy Simulation. *AIAA Journal,* 42(3), pp. 447-456, 2004

[4] Keating, A. and Piomelli, U. and Balaras, E. and Kaltenbach, H.J. A priori and a posteriori test of inflow conditions for large-eddy simulation. *Physics of Fluids,* 16(2), 2004

[5] Shur, M.L. and Spalart, P.R. and Strelets, M.K. and Travin, A.K. Synthetic Turbulence Generators for RANS-LES Interfaces in Zonal Simulations of Aerodynamic and Aeroacoustic Problems. *Flow, Turbulence and Combustion,* 93(1), pp. 63–92, 2014

[6] Schmidt, S. and Breuer, M. Source Term based Synthetic Turbulence Inflow Generator for Eddy-Resolving Predictions of an Airfoil Flow including a Laminar Separation Bubble. *Computers & Fluids,* 146, pp. 1–22, 2017

[7] Becker, K. and Heitkamp, K. and Kügeler, E. Recent Progress In A Hybrid-Grid CFD Solver For Turbomachinery Flows. Proceedings of: *Fifth European Conference on Computational Fluid Dynamics ECCOMAS CFD*, 2010

[8] Roe, P.L. Approximation Riemann Solvers, Parameter Vectors, and Difference Schemes. *Journal of Computational Physics,* 43(2), pp. 357-372, 1981

[9] van Leer, B. Towards the Ultimate Conservation Difference Scheme. V. A Second-Order Sequel to Godunov's Method. *Journal of Computational Physics,* 32(1), pp. 101-136, 1979

[10] Kraichnan, R.H. Diffusion by a Random Velocity Field. *Physics of Fluids,* 13(1), pp. 22-31, 1970

[11] Smagorinsky, J. General circulation experiments with the primitive equations. *Monthly Weather Review,* 91(3), pp. 99-164, 1963

[12] Bergmann, M. and Morsbach, C. and Franke, F. Implicit LES of a turbulent channel flow with high-order discontinuous Galerkin and finite volume discretization. To be published in proceedings of: *ERCOFTAC Direct and Large-Eddy Simulation XI,* 2019

[13] Ducros, F. and Nicoud, F. and Poinsot, T. Wall-Adapting Local Eddy-Viscosity models for simulations in complex geometries. *Numerical Methods for Fluid Dynamics VI,* pp. 293-299, 1998

[14] Iwamoto, K. and Suzuki, Y. and Kasagi, N. Database of a fully developed channel flow. *THTLAB International Report,* ILR-0201, 2002

[15] Batten, P. and Goldberg, U. and Chakravarthy, S. Interfacing Statistical Turbulence Closures with Large-Eddy Simulation. *AIAA Journal 42,* 42(3), pp. 485-492, 2004